INSTITUTE OF PLASMA PHYSICS
CZECHOSLOVAK ACADEMY OF SCIENCES

FLUCTUATION STUDIES ON CASTOR AND ASDEX TOKAMAKS AT LOWER HYBRID CURRENT DRIVE *

Žáček F., Stöckel J., Badalec J., Dvořáček L., Jakubka K., Kletečka P., Kryška L., Magula P., Mlynář J., Söldner F.*, Sizov E. R.**

* This report was presented on IAEA Technical Commitee Meeting on Research Using Small Tokamaks, Hefei, China, October 1991

* IPP Garching

** Institute of General Physics, Moscow

RESEARCH REPORT

IPPCZ - 319 **January 1992**

POD VODÁRENSKOU VĚŽÍ 4, 180 69 PRAGUE 8
CZECHOSLOVAKIA

FLUCTUATION STUDIES ON CASTOR AND ASDEX TOKAMAKS AT LOWER HYBRID CURRENT DRIVE [+]

Žáček F., Stöckel J., Badalec J., Dvořáček L., Jakubka K.,
Kletečka P., Kryška L., Magula P., Mlynář J.,
Söldner F.[*], Sizov E. R.[**]

[+]This report was presented on IAEA Technical Commitee Meeting on Research Using Small Tokamaks, Hefei, China, October 1991

[*]IPP Garching

[**]Institute of General Physics, Moscow

IPPCZ-319

January 1992

Fluctuation studies on CASTOR and ASDEX tokamaks at Lower Hybrid Current Drive *

Žáček F., Stöckel J., Badalec J., Dvořáček L., Jakubka K.,
Kletečka P., Kryška L., Magula P., Mlynář J.,
Söldner F. †, Sizov E.R. ‡

Institute of Plasma Physics
Czechoslovak Academy of Sciences
Pod vodárenskou věží 4, 182 11 Prague 8
Czechoslovakia

Abstract

An improvement of the global confinement is reported from CASTOR and ASDEX tokamaks during lower hybrid current drive (LHCD) regimes at moderate LH powers ($P_{LH} < 1.5P^o_{OH}$, P^o_{OH} is the initial ohmic heating power). Simultaneously a significant reduction of edge electrostatic fluctuations is observed. The best global confinement and the maximum reduction of the edge fluctuations is reached when the total power P_{TOT} delivered into the plasma is minimum ($P_{TOT} = P_{LH} + P^o_{OH}$). Behaviour of the edge plasma parameters, namely the level, frequency spectra and poloidal velocity of electrostatic fluctuations, are documented for CASTOR tokamak.

*This report was presented on IAEA Technical Committee Meeting on Research Using Small Tokamaks, Hefei, China, October 1991

†IPP Garching

‡Institute of General Physics, Moscow

1 Introduction

In present-day tokamaks the experimentally determined energy confinement time is roughly two orders of magnitude lower than the neoclassical prediction. This anomalous transport is generally attributed to the microscopic plasma turbulence, see e.g. a rewiev paper [1], where electrostatic turbulence is identified as the most probably candidate. A large number of theoretical and experimental studies has been devoted to this topic in the last years, however, there are a lot of open questions which have to be still answered.

A direct link between the level of plasma turbulence and global plasma confinement has already been established experimentally in many tokamaks without any doubts. It has been also proved that regimes with the improved confinement (including H-modes), reached under different conditions, are generally characterized by a reduced level of the edge plasma turbulence.

The reduction of edge plasma fluctuations followed by an improvement of global particle confinement has been observed also in tokamak CASTOR [2-4] and tokamak ASDEX as well [5] during the LHCD regimes. In the following a comparison of this observation on both tokamaks is given. Mechanism of such lower hybrid wave effect is not clear, however.

As it was suggested in [6-8] and experimentally investigated in [9-19], an important role in the creation of a transport barrier plays a rearrangement of radial electric field at the plasma edge and the consequent increase of the poloidal rotation velocity in this transport barrier region. This paper gives some experimental evidence about the radial behaviour of these quantities in tokamak CASTOR during the LH wave application. Simultaneously the changes in frequency spectra of edge density fluctuations are discussed.

2 Experimental arrangement

CASTOR tokamak:

Top view of tokamak CASTOR ($R/r_o = 0.4m/0.1m$, $B_T = 1T$, $\tau \leq 50ms$, aperture limiter a=85mm) is given in Fig. 1 together with the most important diagnostics. A multijunction 3-waveguide grill with a broad power spectruml $N_{||} = = 1-4$ was used as a launcher (spectral power density of the wave irradiated by this launcher, enumerated in [20], see the corresponding curve in Fig. 2). A magnetron with the frequency 1.25GHz and power $P_{LH} \leq 40kW \simeq 1.5P^o_{OH}$ is used as a LHW generator (P^o_{OH} is the initial ohmic heating power before the LHW is applied). The experiments were carried out at $I_P = 12kA$ and $\bar{n}_e = 4 - 10 \cdot 10^{18}m^{-3}$. The plasma position was feed-back stabilized.

The global particle confinement time was determined from the plasma density and H_α line intensities in three toroidal positions (at the limiter, at the grill mouth and in the cross-section opposite to the limiter denoted as H_α chamber, see Fig. 1). The line average electronl density $\bar{n}_e$ was measured by a 4mm interferometr, the changes in the density profile $n_e(r)$ were estimated using a measurement along two vertical chords (through the plasma center and at distance 5.4cm from the center)

supposing the density profile in the form $n_e(r) = n_e(0)[1-(r/a^*)^2]^p$. Here $a^* = = 90mm$ was determined by Langmuir probe measurement.

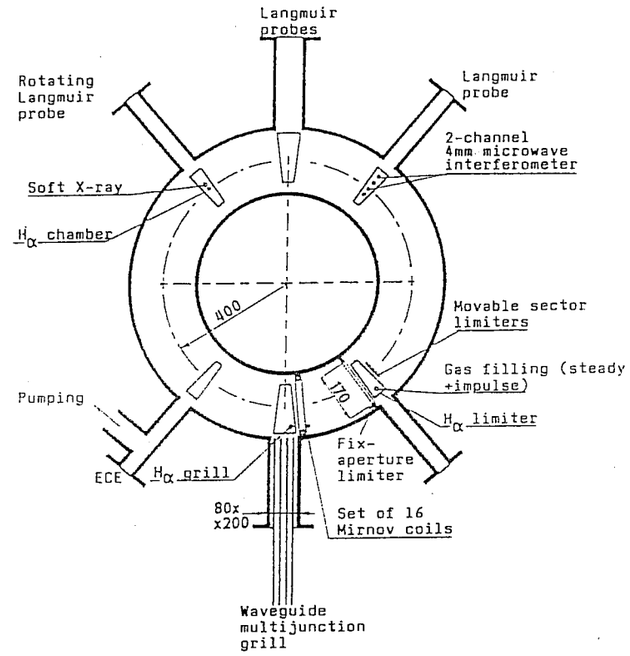

Figure 1: Toroidal geometry of the tokamak CASTOR with schematical set-up of the LH launcher and with the most important diagnostic tools.

Several Langmuir probes, located in the equatorial plane, have been used for measurement of the edge CASTOR plasma:

1. A rotating single probe to determine radial profiles of the floating potential and the ion saturation current during a single shot (placed 135° toroidally away from the grill in the electron drift direction); for more details see [21].

2. Double probes with poloidally separated tips (placed 180° and 225° toroidally away from the grill) for determination of edge plasma turbulent characteristics using a correlation technique.

3. Triple probes for determination of the electron temperature (placed 180° and 225° to the grill).

The radial position of the last two probes could be changed from shot to shot to obtain radial profiles of measured quantities.

The electrostatic fluctuations are investigated either by an analog technique or by digitizing of the probe signals. In the first case, using a three channel

analog correlator [3,22], the rms values of density $\tilde{n}_e$ and poloidal electric field $\tilde{E}_P$ fluctuations as well as the radial turbulent flux Γ, induced by the cross-field drift $E_P \times B_T$, were monitored.

In the second case, the signals are filtered to remove their quasistationary values, processed in the frequency range 0.1-500kHz and digitized by means of A/D convertors with the sampling rate $0.2\mu s$. Afterwards, the correlation functions, frequency spectra and the velocity of the poloidal rotation are determined.

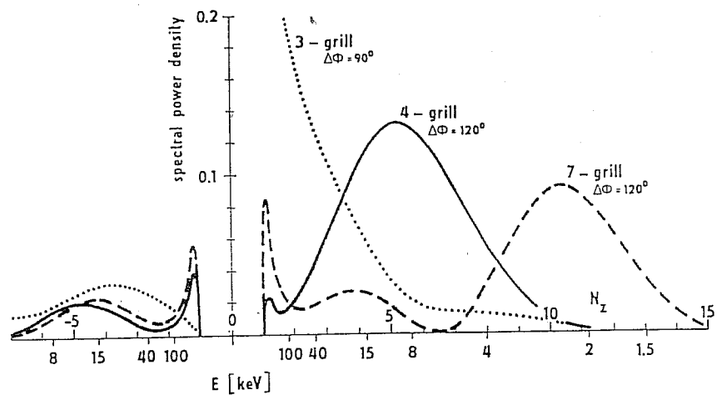

Figure 2: Spectral power densities of the wave irradiated by three types of multijunction grills used for the LH experiments on tokamak CASTOR, enumerated for the plasma density in the grill mouth $3 \times 10^{18} m^{-3}$ with a gradient $10^{20} m^{-4}$.

ASDEX tokamak:

Experiment on tokamak ASDEX ($R/a = 1.65m/0.4m$, $B_T = 2.8T$, $\tau \leq 3s$) has been performed in the LHCD regime with $I_P = 420kA$ ($P^o_{OH} = 390kW$) at frequency 2.45GHz and LH power $P_{LH} \leq 600kW \approx 1.5P^o_{OH}$ (note that the maximum relative value of P_{LH}/P^o_{OH} is the same for both ASDEX and CASTOR tokamaks). The ASDEX LH launcher (phasing 90^o) consists of two independently powered parts (upper and lower grills). The electrostatic fluctuations were monitored by a triple Langmuir probe, located near the equatorial plane, 3cm outside the separatrix and 21^o toroidally away from the LH antenna (the flux tube connected with the probe crosses the front of the lower grill). For their processing the same three channel analog correlator [22] as in the case of tokamak CASTOR was used. Simultaneously, the energy confinement time τ_E was measured.

3 Experimental results

3.1 A link between the edge fluctuations and global confinement in tokamaks CASTOR and ASDEX during LHCD operation

Typical temporal evolution of the LHCD shot on CASTOR tokamak is shown in Fig. 3. It may be seen that the line averaged density $\bar{n}_e$ (Fig. c) increases during the LHCD. Moreover a certain broadening of the radial density profile is observed (d). The gas influx remains unchanged or even slightly decreases (see next figure). Intensities of impurity spectral lines do not increase as well. Therefore, an improvement of the global particle confinement at LHCD can be deduced at least qualitatively. Simultaneously, the level of density fluctuations decreases significantly (i). Similar decrease of potential fluctuations as well as the fluctuation-induced flux at LHCD on CASTOR has already been demonstrated earlier [2].

As follows from temporal evolution of SXR intensities, the signal from the detector with the Al-foils (0.6-1.5 keV) decreases during LHCD by 40-50 %, while the signal from the detector with the Be-foil increases about 10-40 %. Such behaviour can be explained by formation of a tail on the electron distribution function with a temperature $T_{TAIL} \approx 60keV$ and density of about $10^{16} m^{-3}$ [23]. At the same time, the electron temperature of the bulk plasma decreases from $T_e = 135eV$ (OH) to $T_e = 110eV$ during LHCD. It corresponds to results of the determination of T_e by the filters-method.

Evolution of the global particle confinement time is given in Fig. 4. It may be seen that this value (denoted in LHCD regime as τ_{LH}) increases by a factor 2-3 at the LHCD density ramp-up period.

Fig. 5 shows the variation of the relative reduction of the edge density fluctuations $\Delta = (\tilde{n}_{OH} - \tilde{n}_{LH})/\tilde{n}_{OH}$ and the ratio τ_{LH}/τ_{OH} on LH power. It may be seen that both quantities correlate very well and it is worthwhile to note that the maximum effect is reached for such a LH power at which the total power input P_{TOT} is minimum ($P_{TOT} = 0.8P^o_{OH}$).

Fig. 6 demonstrates the link between the relative edge fluctuations of the poloidal electric field and global energy confinement time τ_E in tokamak ASDEX. The similar character of the results obtained on both ASDEX (Fig.6) and CASTOR (Fig.5) tokamaks is striking. Namely, also in the case of much greater tokamak ASDEX, the improvement of the confinement (in this case the confinement of energy; nevertheless, particle confinement exhibites the same features) is the most expressed under such LH power, at which the total power input is minimum ($P_{TOT} = 0.8P^o_{OH}$ again). The fact that this minimum P_{TOT} occurs at relatively lower LH power ($P_{LH}/P^o_{OH} \approx 0.3$) comparing to the tokamak CASTOR ($P_{LH}/P^o_{OH} \approx 0.5$) may be understood through the higher LHCD efficiency in the case of ASDEX.

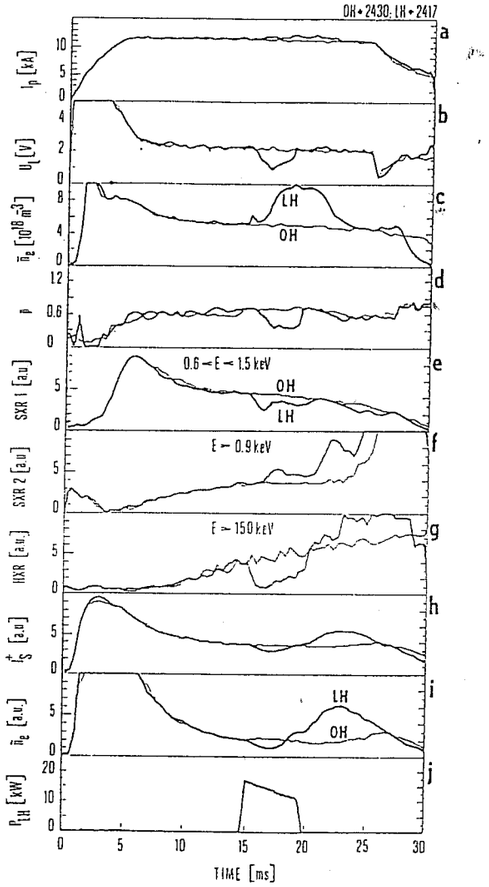

Fig. 3.

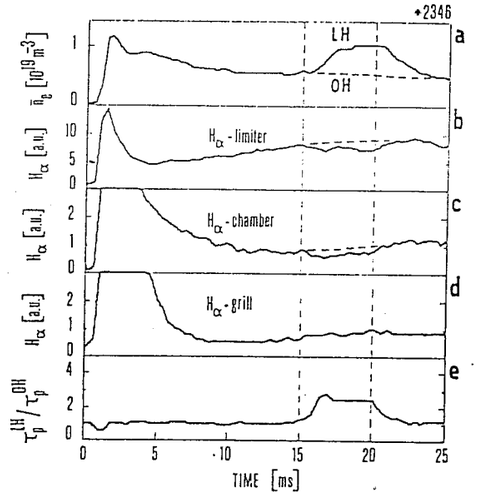

Fig. 4.

Figure 3: Plasma characteristics in OH/LHCD operation of tokamak CASTOR: a) plasma current, b) loop voltage, c) line average density measured along the central chord, d) parameter p characterizing a change in the density profile $n_e(r)$ supposed in the form $n_e(r) = n_e(0)[1 - (r/a^*)^2]^p$ (decrease of p means broadening of the profile), e,f) 2 channels of SXR, g) HXR, h) ion saturation current on the probe in the limiter region, i) density fluctuation measured by this probe, j) LH power.

Figure 4: Temporal evolution of the line averaged density (a), H_α line intensities measured in three toroidally distributed places (b-d) and from these quantities evaluated improvement of global particle confinement time τ_{LH}/τ_{OH} (e); CASTOR, $P_{LH} = 15kW$.

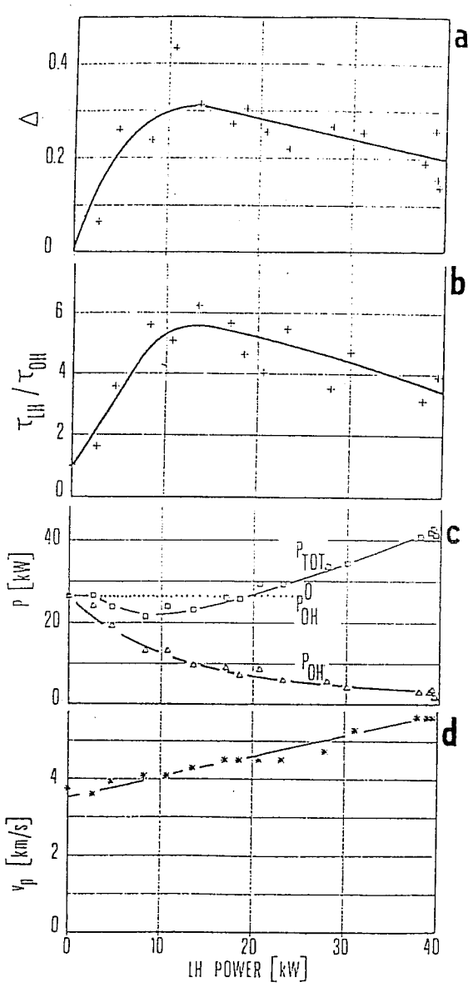

Fig. 5.

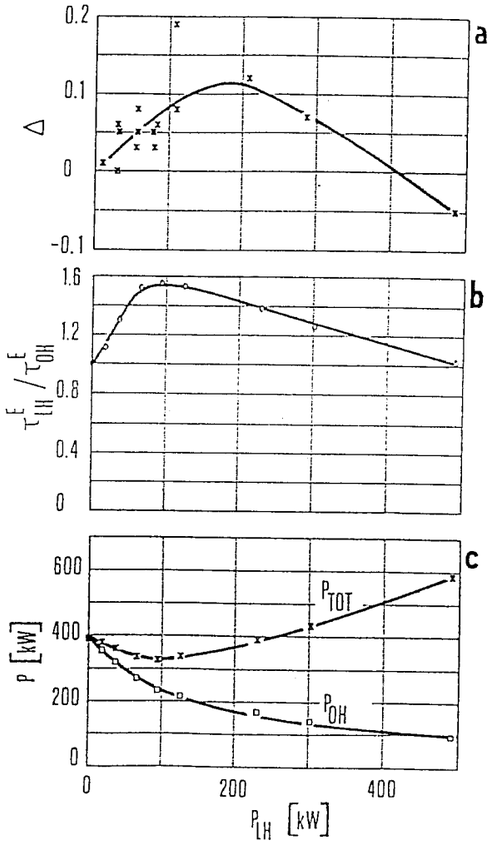

Fig.6.

Figure 5: (a) relative drop of the edge density fluctuations $\Delta = (\tilde{n}_{OH} - \tilde{n}_{LH})/\tilde{n}_{OH}$, (b) relative increase of global particle confinement time τ_{LH}/τ_{OH}, (c) total and residual OH power and (d) velocity of poloidal rotation of the edge density fluctuations measured in tokamak CASTOR at $\bar{n}_e = 6 \times 10^{18} m^{-3}$ in dependence on the input LH power; all values are taken 2ms after the LH power is applied.

Figure 6: (a) relative drop of poloidal electric field fluctuations $\Delta = (\tilde{E}_p^{OH} - \tilde{E}_p^{LH})/\tilde{E}_p^{OH}$, (b) relative increase of global energy confinement τ_{LH}^E/τ_{OH}^E and (c) total and residual OH power measured in tokamak ASDEX at $\bar{n}_e = 1.3 \times 10^{19} m^{-3}$ in dependence on the input LH power; $I_P = 420kA$, $B_T = 2.8T$. Probe position: 3cm outside the separatrix.

3.2 Characterization of the CASTOR edge plasma during LHCD

To understand better the mechanism of fluctuations reduction, the edge plasma was investigated by Langmuir probes in the region $0.97 \leq r/a \leq 1.2$ (a beeing the limiter radius), see Fig. 7.

The electron temperature slightly increases during LHCD but its radial profile remains quite flat near the last closed flux surface (LCFS). Therefore, the radial profiles of I_S and U_f can be roughly interpreted as the profiles of density and space potential. The ion saturation current decreases at LHCD. As the line average density increases and the radial density profile broadens, some steepening of density profile should be expected deeper inside the plasma, i.e. for $r/a < 0.97$. In fact, such steepening during LHCD has been observed earlier on CASTOR by means of the thermal Li beam diagnostics [24]. Note also an increase of the gradient of U_f for $r/a < 1$, which indicate that the radial electric field is more negative at LHCD in this region.

The absolute levels of density and potential fluctuations are reduced throughout the SOL. However, the relative level of density fluctuations decreases only slightly near the LCFS. The same situation is reported for LHCD shots on DITE tokamak [25]. The density fluctuations rotate poloidally in direction of the ion diamagnetic drift and the radial profile of the poloidal velocity changes at LHCD. Note, that the poloidal velocity of density fluctuations increases when $\tilde{n}/n$ is reduced (near LCFS) and vice versa. The close link between these two quantities inside SOL, observed also under different experimental conditions (e.g. at the edge polarisation experiments), is demonstrated in Fig. 8.

In addition, analyzing the fluctuations from the single probe by the Fast Fourier Transform, the frequency spectra of density fluctuations in the laboratory frame can be derived, see Fig. 9a. In general, the form of the frequency spectra changes at LHCD. To characterize these change more quantitatively the autocorrelation function of density fluctuations $R(\tau)$ has been evaluated, see Fig. 9b. The autocorrelation time T is taken as a measure of the width of the frequency spectrum, as T is roughly inversely proportional to the width of the frequncy spectrum [26]. The link of these both quantities can be also seen from brief comparison of Figs. 9a and 9b.

Fig. 10, presenting the variation of the autocorrelation time T with the probe position, shows that near the LCFS the autocorrelation time is shorter in LHCD case ($T_{LH} < T_{OH}$). It implies a broadening of the frequency spectra in the laboratory frame. Going back to Fig. 9a, a reduction of the low frequency part of the spectrum can be seen. Near the wall, on the other hand, the high frequencies are reduced and the frequency spectrum is more peaked with respect to the OH case.

However, the form of the frequency spectrum can be influenced by the poloidal rotation. A simple relation between the autocorrelation time in the laboratory T_{LAB} and in the convected frame T_C is given in [25]: $(1/T_{LAB})^2 = (1/T_C)^2 + (v_p/\lambda)^2$, where λ is the correlation length. To estimate the autocorrelation time in the convected frame a plot of $(1/T_{LAB})^2$ versus the poloidal velocity v_p^2 is given in Fig. 11.

We can see from this figure that the data follow the expression given above.

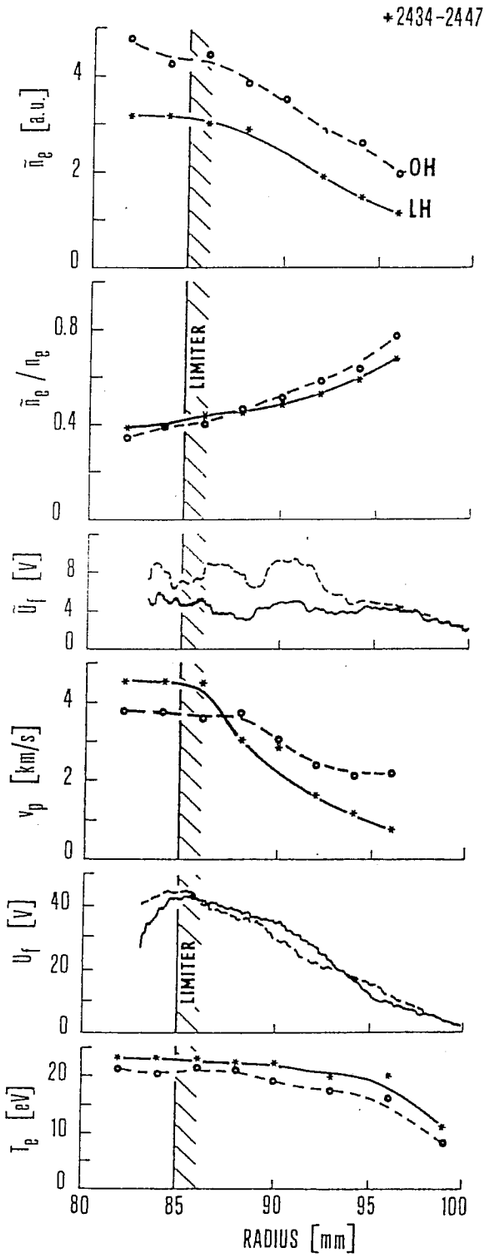

Figure 7: Radial profiles of CASTOR edge plasma characteristics during OH and OH/LHCD discharge phase for $\bar{n}_e = 6 \times 10^{18} m^{-3}$ and $P_{LH} = 20kW$.

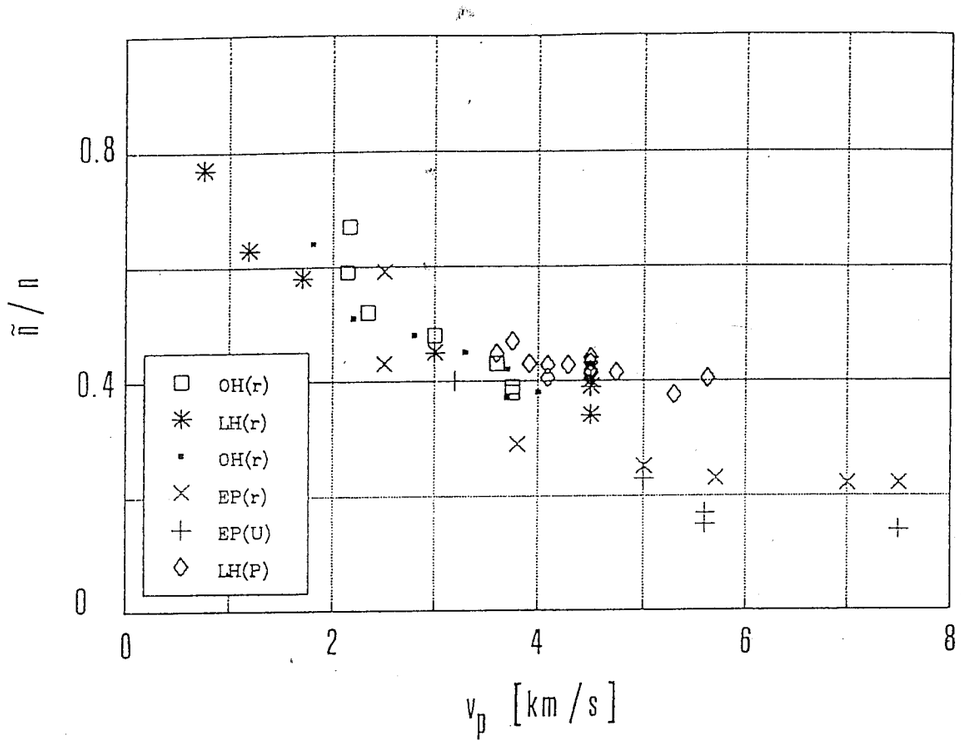

Figure 8: Relation between the relative level of density fluctuations in SOL and their poloidal velocity obtained during measurements of the following dependences:
$OH(r)$ ... radial dependences in OH regimes
$LH(r)$ ... radial dependences in LHCD regimes
$EP(r)$ ... radial dependences in experiments with plasma edge polarization
$EP(U)$ ... dependence on the voltage used for the plasma edge polarization
$LH(P)$ ... dependence on the LHW power.

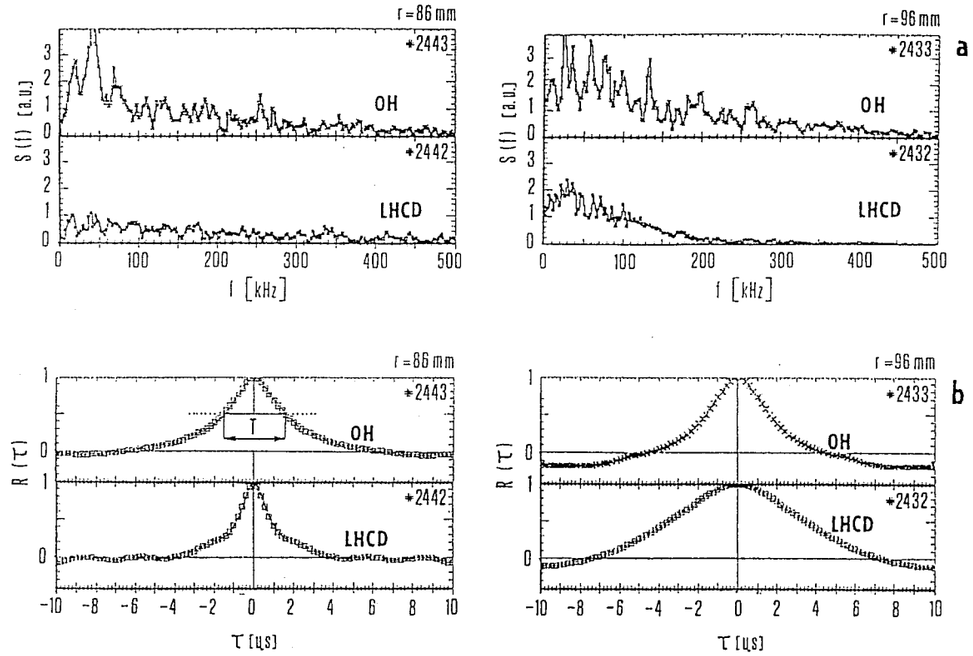

Figure 9: Frequency spectra (a) and autocorrelation functions (b) of density fluctuations measured at two different probe positions r=86 and 96mm in OH and LHCD regimes ($P_{LH} = 20kW$).

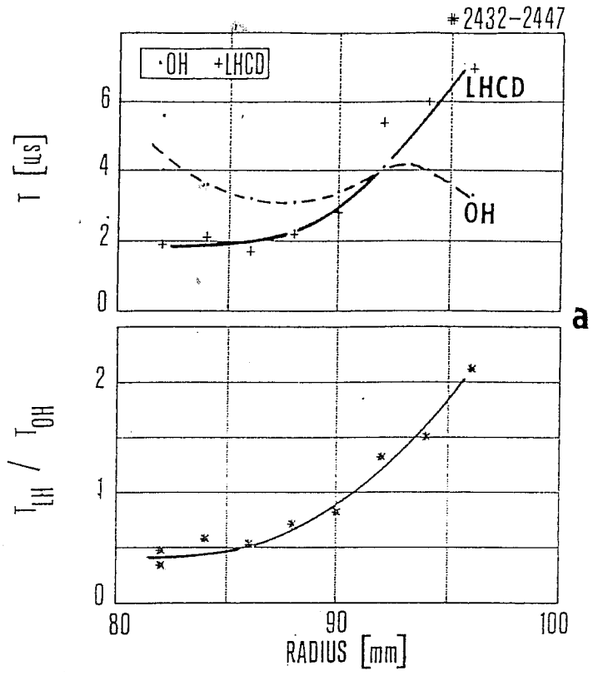

Figure 10: The variation of the autocorrelation time T: a) versus radial position of the probe; b) versus LH power (at r=86mm).

Therefore, an increase of the autocorrelation time T_C in convected frame can be deduced for LHCD case. It suggests a peaking of the frequency spectra. Moreover, the correlation length determined from the slope of the function $(1/T_{LAB})^2 = f(v_p^2)$ decreases from $\approx 1.5cm$ (OH) by a factor of 3-4 during LHCD.

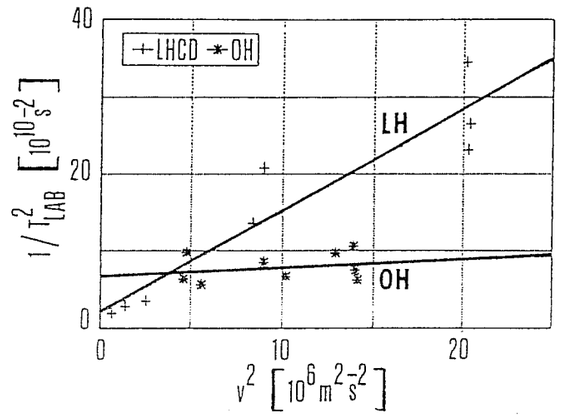

Figure 11: Plot of the autocorrelation time $(1/T^2_{LAB})$ versus poloidal velocity v_P^2.

An interesting results concerning so called "shear layer" existing in the vicinity of the LCFS were obtained in the case of a low density ($\bar{n}_e = 3 \cdot 10^{18} m^{-3}$) discharge without impulse gas puffing. Fig. 12 represents cross-correlation functions of fluctuating signals from the double probe (r=84mm) during OH and LHCD periods of such low density discharge (LH power applied at t=15-20ms). Fig. 13 gives from Fig. 12 evaluated temporal variations of v_P for three different probe radial positions. For comparison two variations in pure OH shots (probe on the radius r=86 and 82mm) are shown in this figure as well. It may be seen, that shear layer staying around the radius r=84mm in the OH phase (limiter radius a=85mm) starts to move outwards during the LHCD.

4 Conclusions

The results, concerning the investigation of the global confinement and the edge plasma turbulence during the LHCD on CASTOR and ASDEX tokamaks, can be summarized as follows:

- An improvement of the global confinement is observed at moderate LH power in the both devices. Simultaneously, a significant reduction of the absolute level of edge electrostatic fluctuations near the LCFS is measured.
- The best improvement of the global confinement and the maximum reduction of fluctuations appears when the total power $P_{OH} + P_{LH}$ delivered into the plasma is minimum.

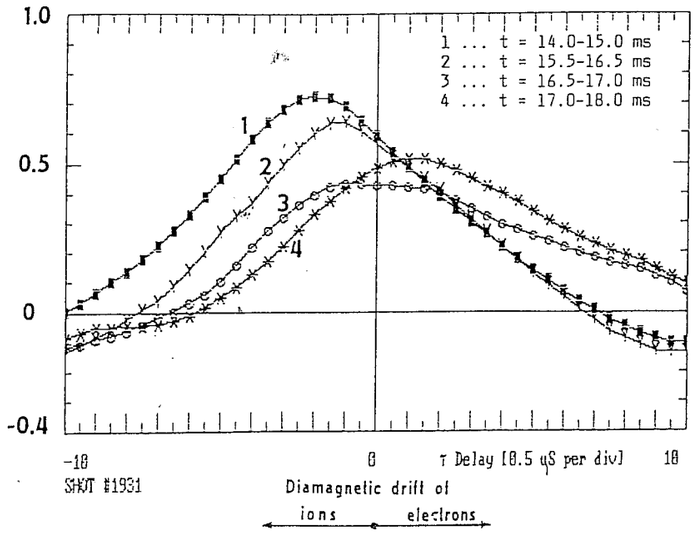

Figure 12: Time evolution of the cross-correlation function of the density fluctuations at the probe radius r=84mm in the LHCD low density regime ($\bar{n}_e = 3 \times 10^{18} m^{-3}$). LH pulse applied at t=15ms.

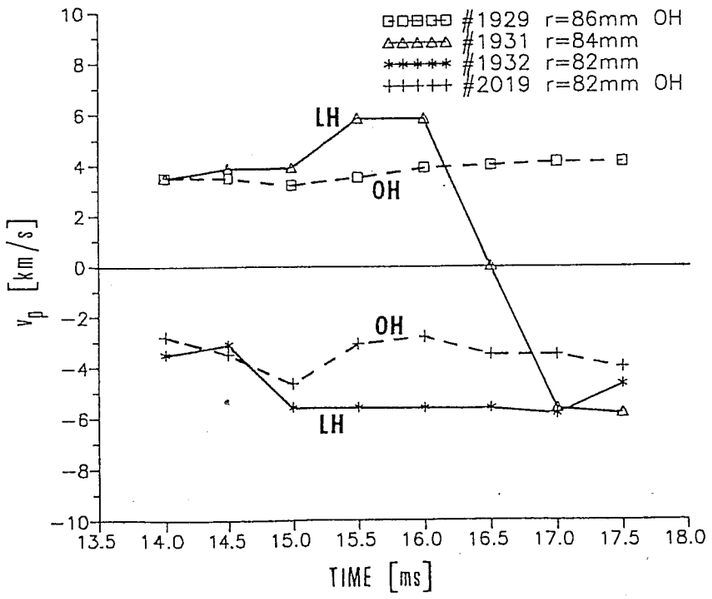

Figure 13: Time evolution of the poloidal rotation velocity of density fluctuations at three different probe radii during the regime shown in Fig. 12.

Moreover, the Langmuir probe data obtained on CASTOR tokamak show following significant changes of edge plasma during the LHCD:

- The radial electric field increases, especially inside the limiter radius.
- A radial shift of the velocity shear layer is observed.
- The increase of the poloidal velocity of density fluctuations in SOL is observed. However, it does not correlate with the improvement of the global confinement generally.
- The local value of the poloidal velocity of density fluctuations seems to be unambiguously related to their relative level $\tilde{n}/n$.
- An internal structure of the edge electrostatic turbulence changes noticeably during the LHCD. Namely, a peaking of frequency spectra and a decrease of correlation length of density fluctuations is observed.

Acknowledgements

The work was performed under Grants of Czechoslovak Academy of Sciences No 14308 and 14310 and was supported also by the IAEA Contract No 6702/RB.

References

[1] Liewer P.C., Nucl. Fus. 25 (1985) 543.

[2] Stoeckel J. et al., 12th Int. Conf. on Pl. Phys. and Contr. Nucl. Fus. Res., Nice 1988, Nucl. Fus. Suppl. 1988, Vol. I, 359.

[3] Stoeckel J. et al., 13th Int. Conf. on Pl. Phys. and Contr. Nucl. Fus. Res., Washington 1990, Proc.I, 491.

[4] Žáček F. et al., 18th EPSC, Berlin 1991, Proc.III, 341.

[5] Stoeckel J. et al., 18th EPSC, Berlin 1991, Proc.I, 249.

[6] Itoh S.I. et al., Phys. Rev. Lett. 60 (1988) 2276.

[7] Shaing K.C. et al., Phys. Fluids B, 2 (1990) 1492.

[8] Rozhanskij V.A. et al., Sov. PZhETP 53 (1991) 80.

[9] Taylor R.J. et al.: Phys. Rev. Lett. 63 (1989) 2365.

[10] Weynants R.R. et al.:. Nucl. Fus. 30 (1990) 945.

[11] Groebner R.J. et al.: Phys. Rev. Lett. 64 (1990) 3015.

[12] Taylor R.J. et al.: IAEA-CN-53/A-6-5, Washington 1990.

[13] Weynants R.R. et al.: IAEA-CN-53/A-6-6, Washington 1990.

[14] Philipona R. et al., 18th EPSC, Berlin 1991, Proc.I, 281.

[15] Gohil P. et al., 18th EPSC, Berlin 1991, Proc.I, 289.

[16] Hidalgo C. et al., 18th EPSC, Berlin 1991, Proc.III, 61.

[17] Tynan G.R. et al., 18th EPSC, Berlin 1991, Proc.III, 89.

[18] Tagle J.A. et al., 18th EPSC, Berlin 1991, Proc.III, 93.

[19] Field A.R. et al., 18th EPSC, Berlin 1991, Proc.III, 113.

[20] Preinhaelter J., Nucl. Fus. 29 (1989) 1729; Czech. J. Phys. 40 (1990) 527: Res. rep. IPPCZ-309, March 1991 (to be publish in Czech. J. Phys.).

[21] Stoeckel J. et al., IAEA Technical Committee Meeting Using Small Tokamaks, Hefei, China, October 1991.

[22] Kryška L. et al., Res. Rep. 22/88, IPP Prague 1988.

[23] Fedorenko S.I. et al., 16th Europ. Conf. on Contr. Fus. and Plasma Research, Part IV, 1267, Venice 1989.

[24] Weixelbaum L. et al., J. of Nucl. Mat. 176& 177(1990) 904.

[25] Vayakis G., Rep. AEA FUS 123, Culham April 1991.

[26] Bendat J.S., Piersol A.G.: "Measurement and analysis of random data", John Wiley & Sons Inc., N.Y. 1967.